

# Three-dimensional model for capillary nanobridges and capillary forces

Alexandre Chau, Stiphane Rignier<sup>2</sup>, Alain Delchambre<sup>1</sup> and Pierre Lambert<sup>1</sup>

<sup>1</sup> Bio Electro and Mechanical Systems, Université libre de Bruxelles, CP 165/14, 50 Av FD Roosevelt, Bruxelles 1050, Belgium

<sup>2</sup> Laboratoire de Robotique de Paris, 18, route du Panorama, Fontenay Aux Roses 92265, France

E-mail: [achau@ulb.ac.be](mailto:achau@ulb.ac.be), [regnier@robot.jussieu.fr](mailto:regnier@robot.jussieu.fr), [adelch@ulb.ac.be](mailto:adelch@ulb.ac.be) and [plambert@ulb.ac.be](mailto:plambert@ulb.ac.be)

Received 5 October 2006, in final form 6 February 2007

Published 26 March 2007

Online at [stacks.iop.org/MSMSE/15/305](http://stacks.iop.org/MSMSE/15/305)

## Abstract

This paper presents a model for the computation of capillary forces (applied to water capillary condensation). For simple geometries (planes, spheres, cones, etc), this model complies well with the literature results. But the literature only provides results for simple shapes and meniscii geometries. Our model allows the computation of capillary force for non-axisymmetrical shapes, with a meniscus fulfilling the Kelvin equation (i.e. we do not assume the profile of the meniscus).

Currently the model takes into account the contact angles, the relative humidity, temperature and the geometrical description of the problem.

The complexity of the problem can result from object shape (modelling for example an AFM tip) and/or from geometrical configuration. Using the model, this article shows that the tilt angle of a tip cannot be neglected when computing capillary forces. It is also shown that the difference between a cone and a pyramid has a significant effect on the computation of the force. The authors propose a simplified formula to determine capillary forces for a range of tips from existing results for similar tips.

Eventually, the paper also shows that this geometrical effect can be used to control the force between a tip and an object, allowing to pick it up and release it.

(Some figures in this article are in colour only in the electronic version)

## 1. Introduction

As miniaturization of objects and systems is further carried on, major problems of manipulation appear, as quoted in the literature [1, 2]. In everyday life, when picking up an object, the major opposing force is gravity, which is a volume force. With objects downscaling, surface forces become more and more important and the major opposing force to picking up and releasing

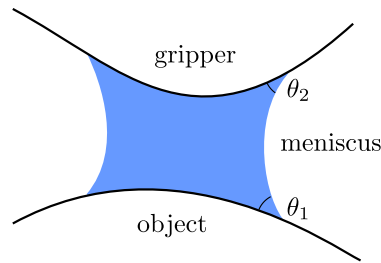


**Figure 1.** Scheme of the problem: a tip and an object are linked by a liquid meniscus, due to humidity condensation; the major non-geometrical parameters are the contact angles  $\theta_1$  and  $\theta_2$  and the surface tension  $\gamma_{lv}$  of the liquid–air interface (here the liquid is always water)

parts becomes adhesion [3]. The force needed to separate two objects is also known as pull-off force. Adhesion is also a major force when considering the interactions between micro- and nanoparticles.

The adhesion force is actually composed of different forces: electrostatic force, van der Waals force, chemical forces and capillary force. Electrostatic force can be avoided by properly choosing materials. van der Waals force arises from the intrinsic constitution of matter: it is due to the presence of instantaneous dipoles. It becomes non-negligible under the nanometer scale. Chemical forces are due to the bondings between particles. It is active when objects are in contact (i.e. the distance between them is about an intermolecular distance).

Capillary force between two objects is due to the presence of liquid between them (see figure 1). On a macroscopic scale, it has already been shown [4] that it can be used to manipulate small objects (300–500  $\mu\text{m}$  of characteristic dimensions) by manually placing a liquid droplet on the object (a fraction of  $\mu\text{l}$ ). This paper aims at theoretically studying the feasibility of manipulating smaller (50–100  $\mu\text{m}$  of characteristic dimension) objects using capillary condensation, i.e. without placing a droplet.

In assembly, it is as important to pick up as it is to release the object: the force applied onto the object should therefore be controllable. It is here proposed to control the force by tilting the tip (an application could be an AFM tip) with respect to the object. Models that assume objects and meniscus to be axially symmetrical [5,6] therefore become inapplicable. A more general model has thus been developed to compute the capillary force without this constraint of axisymmetry.

This paper is organized as follows: first, the basic equations are recalled (section 2) and their validity discussed (section 3). The model implemented in our simulation is then presented (section 4). Finally, results are explained (section 5) and discussed (section 6) for different cases: first axisymmetrical shapes are used only for the purpose of validation, then more complex configurations are studied.

## 2. Equations

### 2.1. Introduction

This section details the different equations involved in the problem :

- the Kelvin equation [7], which rules the curvature of the liquid meniscus and
- the approaches encountered in the literature to compute the capillary force, i.e.
  - the Laplace approach, based on direct force calculations and
  - the energetical approach, based on the derivation of the total energy of the interfaces.

In all the cases, gravity is neglected. This will be valid as long as the dimensions of the meniscus are much smaller than 1 mm.

The current paper only provides results for capillary forces: this is on the assumption that the influence of the van der Waals forces can be neglected. Following the works of Bowden and Tabor [8], de Boer *et al* [9] and van Spengen *et al* [10], for silicon, the total interaction energy is dominated by capillary forces at high humidity levels (above 70–80% humidity). For silicon with 3 nm rms surface roughness, the van der Waals interaction energy is about  $10^{-5} \text{ J m}^{-2}$ , while at 80% RH and  $20^\circ\text{C}$ , the surface interaction energy is about  $10^{-1} \text{ J m}^{-2}$ .

## 2.2. Kelvin equation

In any method used to compute the capillary force, the meniscus shape appears explicitly or implicitly. In the Kelvin equation approach, it is involved through the total mean curvature  $H$  of the meniscus, or its inverse  $r$ , the mean curvature radius

$$H = \frac{1}{r} = \frac{1}{2r_K} = \frac{1}{2} \left( \frac{1}{r_1} + \frac{1}{r_2} \right), \quad (1)$$

where  $r_K$  is, in the case of capillary condensation, the so-called Kelvin radius, and  $r_1$  and  $r_2$  are the two principal curvature radii. The Kelvin radius is dependent on environmental and materials properties and can be computed with the Kelvin equation [3], which is the fundamental equation for capillary condensation

$$r_K = \frac{\gamma V_m}{RT \log_e(p/p_0)}, \quad (2)$$

where  $V_m$  is the molar volume of the liquid,  $R$  is the perfect gas constant ( $8.31 \text{ J mol}^{-1} \text{ K}^{-1}$ ),  $T$  is the temperature (in kelvin) and  $p/p_0$  is the relative humidity (RH), between 0 and 1. Typically, for water, this gives  $r_K = 0.54 \text{ nm} / \log_e(RH)$ , which gives for  $\text{RH} = 90\%$ , a Kelvin radius of about 5 nm at  $20^\circ\text{C}$ .

## 2.3. Laplace approach

With this method, the capillary force is split into two components, the Laplace force and the surface tension force [7].

It must be pointed out here that, in the general case, the force has no reason to be directed only along the axis of the distance between objects. It must be expressed as a vector. Actually, the Laplace approach described here implicitly assumes that the meniscus (and the tip and the object) is axisymmetrical. Only one component is then different from zero. Consequently, this methodology cannot be applied in the general case, at least in the simple form presented here.

The Laplace force is due to the pressure difference  $\Delta p = p_{\text{in}} - p_{\text{out}}$  across the liquid–vapour interface. Using the so-called Laplace equation, it can be expressed as [7]<sup>3</sup>

$$F_L = -\Delta p A = -2 \gamma H A, \quad (3)$$

where  $\gamma$  is the liquid–vapour interface surface tension,  $H$  is the total mean curvature of the meniscus and  $A$  is the area of contact between the meniscus and the object.  $A$  is actually the effective area, i.e. the projection of the wetted interface onto a plane perpendicular to the force.

The other component of the capillary force is due to the surface tension of the liquid–object interface. Considering this surface tension as a constant

$$F_T = L \gamma \sin \theta, \quad (4)$$

<sup>3</sup> Note the sign of the force : here, the force is positive if attractive.

where  $L$  is the perimeter of the liquid–object interface, and  $\theta$  the liquid object contact angle (this contact angle is supposed to be constant).

The capillary force is thus given by

$$F = -2 \gamma H A + L \gamma \sin \theta. \quad (5)$$

Note that  $F_T$  is always attractive, while  $F_L$  can be either attractive or repulsive depending on the sign of the mean curvature.

The calculation can also be conducted on the meniscus/tip interface, the result will obviously be the same.

Different approximations are usually made to this latter equation, which will be detailed in section 2.3.1.

**2.3.1. Usual approximations.** When the equations to obtain the capillary force are developed, a second order differential equation arises. Equation (6) is the full development of the equation, on the assumption of axisymmetrical meniscus to reduce the order of the equation.

$$\frac{\Delta p}{\gamma} = -\frac{r''}{(1+r'^2)^{3/2}} + \frac{1}{r(1+r'^2)^{1/2}}. \quad (6)$$

Usually, the shape of the objects is limited to simple analytical functions, such as planes, spheres, cones or paraboloids to obtain easier boundary conditions.

To further simplify the problem, some authors assume the shape of the meniscus *a priori*: arc of circle, parabola, etc [5, 11, 12]. It will be further shown (section 5) that the circular approximation gives satisfactory results in many cases.

Nevertheless, as the easiest way of controlling the force is to tilt one of the objects, the axisymmetry assumption is not valid anymore and the general equation has to be solved.

#### 2.4. Energetical view

The same results can be obtained via an energetical approach. The total energy of the meniscus can be expressed as

$$W = \gamma_{LV}A_{LV} + \gamma_{LO}A_{LO} + \gamma_{LT}A_{LT} + \gamma_{OV}A_{OV} + \gamma_{TV}A_{TV}, \quad (7)$$

where  $\gamma_{ij}$  is the surface tension of the  $i$ – $j$  interface : **L**iquid, **V**apor, **O**bject and **T**ip and  $A_{ij}$  are the areas of these interfaces. Note that here, the areas are the actual areas and not the effective areas.

The capillary force in the  $z$  direction can then be computed using a classical derivative of the energy with respect to the distance between the objects. If the problem is axisymmetrical, the  $z$  direction is the axis of symmetry, otherwise it can be any direction along which the force is calculated<sup>4</sup>.

$$F = \frac{dW}{dz}. \quad (8)$$

It can be shown that both formulations (Laplace approach and energetical approach) presented here are equivalent and obviously should lead to the same results. The model presented in this paper uses the energetical approach, as will be explained later.

<sup>4</sup> Once again, a positive force means attraction

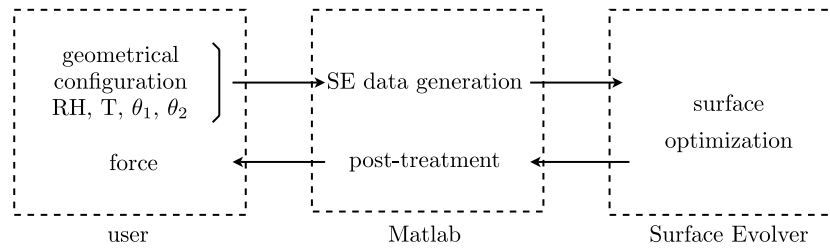


Figure 2. Diagram of the model.

### 3. Validity of the equations

Both the methods presented here are based on a macroscopic hypothesis on the nature of the liquids and solids: matter is continuous and so are their properties such as surface tension. It has been experimentally shown that those models are valid down to menisci of radii as small as 4 nm [13]. For smaller sizes, the discrete nature of matter should be taken into account, via molecular dynamics or Monte-Carlo calculations [14]. The results will thus have to be interpreted keeping in mind that their validity is not proven for very small sizes of meniscus (i.e. for meniscus with radii < 4 nm).

Another discussion encountered in the literature is the parameter kept constant during the derivative: should it be computed keeping the volume or the curvature constant [15]? Different mechanisms play a role here, mainly the condensation/evaporation rate. The literature shows that the condensation takes place in the millisecond (< 5 ms [15]) scale while the evaporation needs more time: meniscus stretching at tip-object distance much larger than  $r_K$  have been measured [15]. Capillary condensation also has a long-term (up to tens days) component, which is not considered here [16].

If experimental investigation could provide an estimation of the characteristic times involved in the processes, it would seem natural to compute the volume condensed—fulfilling the Kelvin equation—at the smallest tip-object distance and then compute the evolution of the force with constant volume when retracting the tip.

### 4. Model and simulation scheme

It is necessary to handle non-axisymmetrical menisci, for example, to quantify the effect of geometrical differences with ideal case or to deal with complex shapes. As the equations in the general case cannot be solved analytically, a numerical model has been developed, which allows the user to define three-dimensional shapes, with some limitations though, which are presented below.

The solver uses the software Surface Evolver (SE) [17]. The total energy of the meniscus is minimized, fulfilling the Kelvin equation. The energy is then derived (by finite differentiation) in the desired direction (usually the distance between objects, but this is not mandatory) to obtain a component of the force acting between the objects (see figure 2).

#### 4.1. Available shapes

The goal of this model is to allow the user to easily compute the capillary force between two objects with parameters unavailable for usual axisymmetrical models. The choice was made to keep a reference axis  $z$ , similar to the symmetry axis of former models.  $z$  will be an axis parallel to the direction of the movement of the tip.

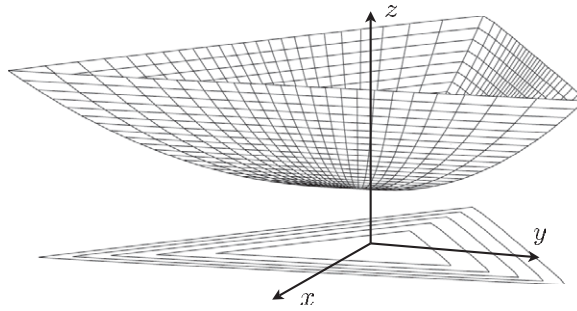


**Figure 3.** Example of a tip and its projection on the  $(x, y)$  plane. Here, the section is a triangle and the profile is a parabola.

To develop complex shapes without defining each point of the tip (or the object), analytical shapes have been used. In the  $z$  direction, usual profiles can be chosen: circular, conical or parabolical, while in the  $(x, y)$  plane, the section of the tip can be described as a polar function.

Elementary sections are

- circle:  $r(\theta) = R$ ,
- triangle:  $r(\theta) = c/(2\sqrt{3} \cos \theta)$  for  $-\pi/3 < \theta \leq \pi/3$  and
- square:  $r(\theta) = c/(2 \cos \theta)$  for  $-\pi/4 < \theta \leq \pi/4$ .

In a similar way, any regular polygon of side length  $c$  can be very easily implemented. Actually, virtually any section can be represented as it is developed in Fourier series (in polar coordinates) in order to obtain an analytical shape on the domain  $\theta = [0; 2\pi]$ .

The profile and the section are then coupled to obtain the complete tip that has to be used in the equations. An example of a tip with parabolic profile and triangular section is shown in figure 3. The same formulation is also available for the object.

This model can be applied to actual commercial tips, such as AFM tips.

## 5. Results

### 5.1. Introduction

The results presented in this section are twofold. First, the validity of the code will be shown in section 5.2. As the literature only provides results for axisymmetrical shapes, these results will be the only ones that can be used as a proof for the model, since no result is available for other shapes.

Then, in sections 5.3 and 5.4, more complex shapes will be investigated.

### 5.2. Validation

Benchmark results used for comparison are separated into three groups:

- Exact solution: analytical solution [6, 18].
- Assumed shape meniscii [5, 11].
- An experimental study [19],

In [6], analytical solutions are derived from the basic equations. They provide results for the sphere–plane and sphere–sphere cases separated by a liquid bridge. The results (see figure 4) are presented with respect to the so-called filling angle  $\psi$  (see inner scheme).

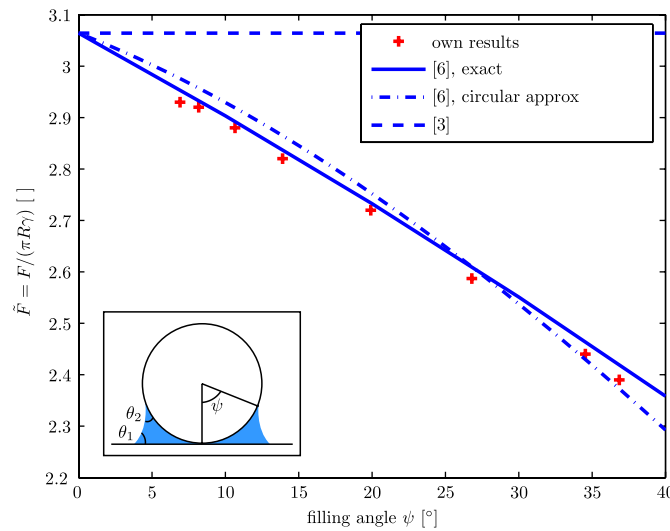


**Figure 4.** Comparison of capillary force at the contact between a sphere and a plane for several models ( $\theta_1 = \theta_2 = 40^\circ$ ). The positive value of force means an attractive force.

One can see that the correspondence is very good with the model from [6] and that the approximation of [3] ( $F = 4\pi R\gamma \cos \theta$ ) is valid for very small angles.

The discrepancies between the model results and [6] can be explained by the meshing of the meniscus. The mesh has to be limited to keep the computation time within acceptable boundaries. In general, the total computation time for a configuration is in the 1–5 min range.

In [5], the shape of the tip is a parabola. The force values coincide well. We choose here to show the shape of the meniscus (see figure 5). It can be seen that—in the axisymmetrical case—the circle approximation for the meniscus shape is valid under the considered conditions (see figure caption).

References [11] and [18] also present the capillary force for different tip shapes (spheres, paraboloids). Again, the results of the model are as close as for the other ones.

Reference [19] presents a theoretical and experimental study on the adhesion between two spheres (see figure 6). It must be noted that here, capillary forces are due to liquid that is not condensed but intentionally placed. Again, one can note the good correspondence between the model and the measurements.

### 5.3. Effect of the tip shape

The model proposed here allows to compute the influence of the tip shape on the force. A comparison of the capillary force between a cone and a plane, a triangular pyramid and a plane and a square pyramid and a plane is presented in figure 7. The parameter is the aperture angle  $\alpha$  of the tip.

As can be seen in figure 7, all other things being equal, the force can be written in the form

$$F = k(\tan \alpha)^n. \quad (9)$$

This result allows us to calculate the force between a tip and a plane, with the knowledge of another tip of the same type. The parameters  $k$  and  $n$  have to be fitted to a set of initial computations/measurements.

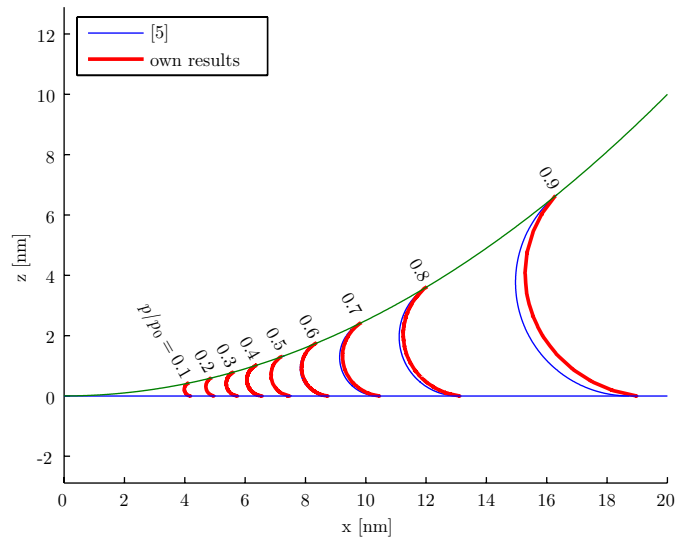


**Figure 5.** Comparison of capillary menisci between a paraboloid (of curvature radius 20 nm at the apex) and a plane for our model and the model from [5].  $\gamma = 72.5 \text{ mN m}^{-1}$ ,  $\theta_1 = \theta_2 = 0^\circ$ .

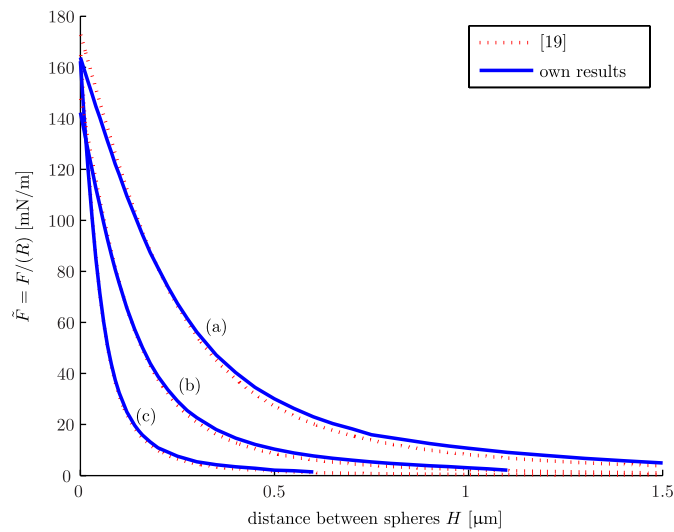


**Figure 6.** Comparison of the presented model with experimental results of Rabinovich [19]. Parameters used :  $R_1 = 19 \mu\text{m}$ ,  $\theta = 10^\circ$ , (a)  $R_2 = 27.5 \mu\text{m}$ ,  $\gamma = 28 \text{ mN m}^{-1}$ ,  $V = 2 \text{ nm}^3$ ; (b)  $R_2 = 32.5 \mu\text{m}$ ,  $\gamma = 24 \text{ mN m}^{-1}$ ,  $V = 12 \text{ nm}^3$  and (c)  $R_2 = 35 \mu\text{m}$ ,  $\gamma = 27 \text{ mN m}^{-1}$ ,  $V = 36 \text{ nm}^3$ .

Another observation is that there is a significant difference between a cone and a triangular/square pyramid. The ratio  $F_{\text{cone/triangular pyramid}} \approx 2.6\text{--}2.8$ , while  $F_{\text{cone/square pyramid}} \approx 7$  with the chosen parameters.

Another comparison is shown in figure 8. Again, the force between a cone and a plane is compared with the force between a triangular pyramid and a plane. Here, the parameter is the relative humidity.



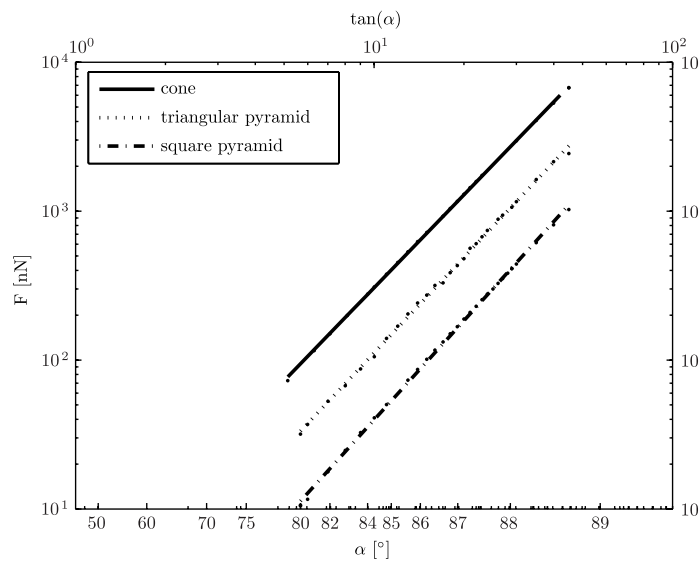


**Figure 7.** Comparison of the capillary force between a cone, a triangular pyramid, a square pyramid and a plane.  $RH = 90\%$ ,  $T = 298$  K, both contact angles are of  $30^\circ$ .  $\alpha$  is the aperture angle of the cone or pyramid; for the pyramids, the aperture angle is the angle between the ‘axis’ of the pyramid and one of the edges.

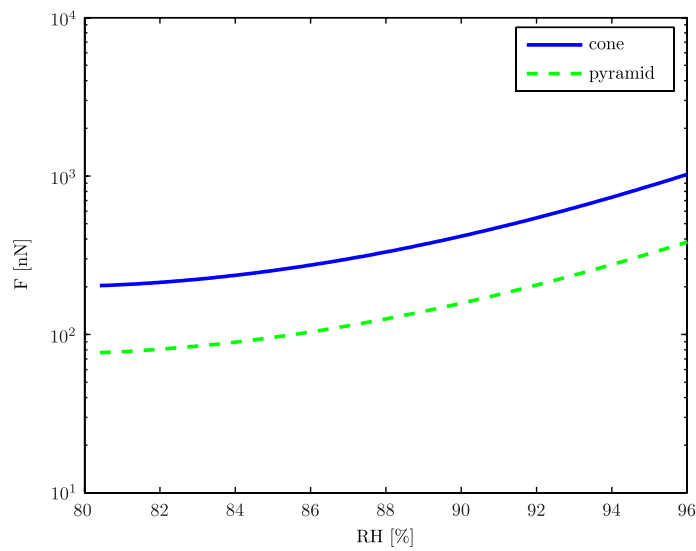


**Figure 8.** Comparison of the capillary force between a cone, a triangular pyramid and a plane.  $\alpha = 80^\circ$ ,  $T = 298$  K, both contact angles are  $30^\circ$ .

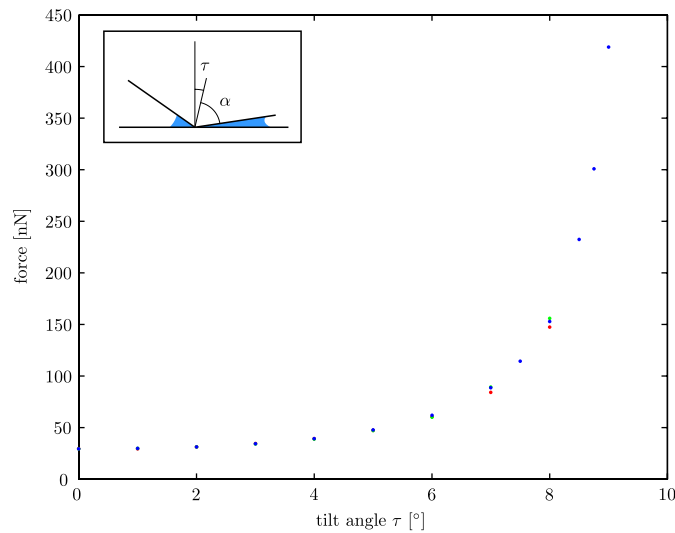


**Figure 9.** Force between a tilted tip (the tilt angle is  $\tau$ ) and a plane. The aperture angle of the cone ( $\alpha$ ) is  $80^\circ$ , temperature is 298 K and the relative humidity is 90%. Both contact angles are of  $30^\circ$  and the surface tension is  $72 \text{ mN m}^{-1}$ . The positive value of force means an attractive force. The different points at the same tilt value are for different mesh refinements. They give an idea of the numerical uncertainty on the results.

Here, a linear relation is not sufficient. The important observation is that the same significant difference between the shapes remains. The ratio  $F_{\text{cone/pyramid}} \approx 2.6\text{--}2.8$  at any point of the curve.

#### 5.4. Tilted tips

In addition to the already existing results, our model is able to compute the capillary force for additional configurations, as detailed in section 4.1.

An important result, which can be achieved with non-axisymmetrical tips is the evolution of the capillary force with the tilt angle of the tip with respect to the object. Figure 9 shows the influence of the tilt angle  $\tau$  on the force for a conical tip.

The conical tip for which the results are presented has an aperture angle  $\alpha$  of  $80^\circ$  (the tilt angle is thus limited to a maximum of  $90^\circ - 80^\circ = 10^\circ$ ). One can see that the force can vary from about 30 nN to over 400 nN, simply by tilting the tip over the plane. In theory, the maximum force could be infinite, but it is in practice limited by the size of the tip, surface roughness and validity of continuum hypothesis for very thin water layers.

Previous results for a cone can be compared with the results of different paraboloids (the parameter  $R$  is the tip radius). Figures 9 and 10 are not combined as geometrical parameters are different. Three different tip radius are investigated in figure 10.

One can see that for the same angle range, the relative variation of the force is reduced compared with the perfect cone. This is discussed in the next section.

## 6. Discussion

In the previous paragraphs, it was shown that our model could be used to compute the capillary force between two objects for the usual shapes: planes, spheres, cones, etc and

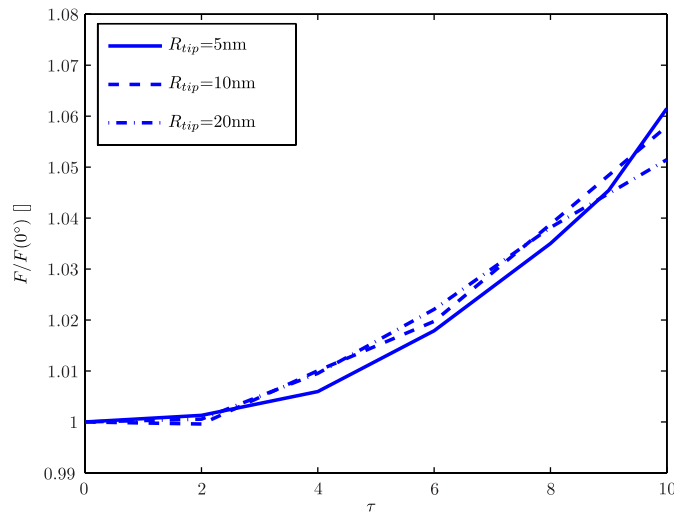


**Figure 10.** Force between tilted paraboloids (the tilt angle is  $\tau$ , see previous figure) and a plane. Temperature is 298 K, the relative humidity is 90%. Both contact angles are  $30^\circ$  and the surface tension is  $72 \text{ mN m}^{-1}$ . The force is reduced to its value at  $\tau = 0^\circ$ .

reproduce existing results. In addition, the three-dimensional capabilities of the model allow the user to compute the capillary force for complex configurations with simple shapes or even with complex shapes (e.g. pyramids, rounded pyramids that can model the Berkovich AFM tips).

A very interesting result presented in the previous section is that the force between the tip and the particle can be controlled by tilting the tip; the force can be multiplied or divided by a factor of more than 10. This ratio should allow the user to pick up and release a particle by controlling the tilt angle of the tip with respect to the object. Note that the force reduction during the part release needs the evaporation of the liquid. This could take some time, as mentioned in section 3.

To fix an order of magnitude, and with the geometries chosen, the minimum and maximum forces are sufficient to lift, respectively, a cube of about 50 and  $100 \mu\text{m}$  for a density of  $2300 \text{ kg m}^{-3}$  (approximately density of silicon). For objects with masses between those values, a conical tip should be able to pick up and then release them in atmospheres of 90% humidity.

One can see that for paraboloids, the relative effect on the force was diminished. An explanation is that for small tilt angles, the meniscus shape variation for the cone is very significant, while it is limited for curved tips. With real tips, one should observe the paraboloid behaviour if the meniscus is too small to expand beyond the rounded zone of the tip while the conical behaviour should be observed for large meniscus (i.e. high humidity). Nonetheless, it is obvious that the more similar to a sphere the tip is, the more the force will be independent of the tilt angle.

Another result presented here was the comparison between the force between a cone and a plane and that between a pyramid and a plane. It is interesting to note that all other things being equal, a cone/pyramid ratio can be determined. It could allow us to compute the force for one geometry and infer the value of the force for the other ones. The significant difference of the force between different shapes arises from the differences in the meniscii shapes. It was shown (see section 2.3) that the capillary force can be computed if the contact area and the contact line length of one of the two solid–liquid interfaces are known. For a pyramid

and a cone of the same aperture angle, both the contact area and the contact line length are significantly smaller for the pyramid-plane case than for the cone-plane case. However, the ratio cannot be determined with such simple arguments and has to be computed.

The next step in the use of the model is its experimental validation. Even though our model complies with the other literature benchmarks, new results obviously cannot be compared with existing ones. Experiments will thus be needed to validate the exactitude of our results. Another contribution that could come out of the experiments is the choice between the constant curvature and constant volume hypothesis, considering different speeds for the approach and retraction of the tip.

In the experiments it is necessary to be able to distinguish capillary forces from van der Waals forces. Here van der Waals forces are not investigated, and the experiments will have to eliminate them from the results, e.g. by working at different relative humidities.

## 7. Conclusions

This paper presented a three-dimensional model for the computation of the capillary force. It allows us to compute the effects of capillary condensation, in configurations that are not mandatorily axisymmetrical. The model has been validated by comparing it with existing theoretical and experimental results. New applications were then proposed:

- it was shown that forces between a pyramid and a plane are significantly smaller than those between a cone (of the same aperture angle as the pyramid) and a plane, and that this ratio did not have a significant dependence on humidity;
- it was also shown that the tilt angle of the tip had a significant effect on the capillary force (the studied conical configuration showed that it should be possible to pick up and then release objects which are bound to the substrate with a force of 100–500 nN). The amplitude of this tilt effect also has a strong dependence on the tip and particle shapes, due to the strong dependence of the force on the geometry.

In the next step, AFM experimental results will have to validate those numerical results. As quoted in the discussion, van der Waals forces were not investigated here. A similar work on these forces could be useful to determine their influence and try to use them for low humidity levels.

## Acknowledgment

This work is funded by a grant from the *F.R.I.A.—Fonds pour la Formation à la recherche dans l'industrie et l'agriculture*.

## References

- [1] Mastrangelo C H 1993 *J. Microelectromech. Syst.* **2** 33–43
- [2] Wu D, Fang N, Sun C and Zhang X 2006 *Sensors Actuators A* **128** 109–15
- [3] Israelachvili J N 1992 *Intermolecular and Surface Forces* 2nd edn (New York: Academic)
- [4] Lambert P, Seigneur F, Koelemeijer S and Jacot J 2006 *J. Micromech. Microeng.* **16** 1267–76
- [5] Stifter T, Marti O and Bhushan B 2000 *Phys. Rev. B* **62** 13667–73
- [6] Orr F M, Scriven L E and Rivas A P 1975 *J. Fluid Mech.* **67** 723–42
- [7] Adamson A W and Gast A P 1997 *Physical Chemistry of Surfaces* 6th edn (New York: Wiley) ISBN 0471148733
- [8] Bowden F P and Tabor D 1954 *The Friction and Lubrication of Solids* 2nd edn (Oxford: Clarendon)
- [9] de Boer M P, Knapp J, Mayer T and Michalske T 1999 *SPIE/EOS Conf. on Microsystems Metrology and Inspection (Munich)* (Bellingham, WA: SPIE Optical Engineering Press)

- [10] Van Spengen W M, Puers R and Wolf I D 2003 *J. Adhes. Sci. Technol.* **17** 563–82
- [11] de Lazzer A, Dreyer M and Rath H J 1999 *Langmuir* **15** 4551–9
- [12] Pepin X, Rossetti D, Iveson S M and Simons S J R 2000 *J. Colloid Interface Sci.* **232** 289–97
- [13] Fisher L R and Israelachvili J N 1981 *Colloids Surf.* **3** 303–19
- [14] Jang J, Ratner M A and Schatz G C 2006 *J. Phys. Chem. B* **110** 659–62
- [15] Sirghi L, Szoszkiewicz R and Riedo E 2006 *Langmuir* **22** 1093–8
- [16] Restagno F 2000 Interactions entre contacts solides et cinétique de la condensation capillaire. Aspects macroscopiques et aspects microscopiques *Ph.D. Thesis* Ecole Normale supérieure de Lyon Lyon
- [17] Brakke K 1992 *Exp. Math.* **1** 141–65 <http://www.expmath.org/restricted/1/1.2/brakke.ps.gz>
- [18] Pakarinen O H, Foster A S, Paajanen M, Kalinainen T, Katainen J, Makkonen I, Lahtinen J and Nieminen R M 2005 *Modelling Simul. Mater. Sci. Eng.* **13** 1175–86
- [19] Rabinovitch Y I, Esayanur M S and Mougdil B M 2005 *Langmuir* **21** 10992–7